

Pairing in graphene: A quantum Monte Carlo study

Tianxing Ma,^{1,2} Zhongbing Huang,^{3,2,*} Feiming Hu,⁴ and Hai-Qing Lin^{2,4,†}

¹*Department of Physics, Beijing Normal University, Beijing 100875, China*

²*Beijing Computational Science Research Center, Beijing 100084, China*

³*Faculty of Physics and Electronic Technology, Hubei University, Wuhan 430062, China*

⁴*Department of Physics and ITP, The Chinese University of Hong Kong, Hong Kong*

(Dated: August 24, 2018)

To address the issue of electron correlation driven superconductivity in graphene, we perform a systematic quantum Monte Carlo study of the pairing correlation in the $t - U - V$ Hubbard model on a honeycomb lattice. For $V = 0$ and close to half filling, we find that pairing with $d + id$ ($d_{x^2-y^2} + id'_{xy}$ in its specific form) symmetry dominates pairing with extended- s symmetry. However, as the system size or the on-site Coulomb interaction increases, the long-range part of the $d + id$ pairing correlation decreases and tends to vanish in the thermodynamic limit. An inclusion of nearest-neighbor interaction V , either repulsive or attractive, has a small effect on the extended- s pairing correlation, but strongly suppresses the $d + id$ pairing correlation.

Recently, graphene has attracted the attention of experimentalists and theorists¹⁻⁴. One of the most intriguing properties of graphene is that its chemical potential can be tuned through an electric field effect, and hence it is possible to change the type of carriers, electrons, or holes, opening the doors for carbon based electronics^{2,5,6}. Doped graphene has a finite density of state at the chemical potential, which, in combination with pronounced antiferromagnetic (AFM) spin fluctuations close to half filling^{7,8}, may lead to an unconventional superconductivity. Experimentally, superconducting (SC) states in graphene have been realized by the proximity effect through contact with SC electrodes⁹, which indicates that Cooper pairs can propagate coherently in graphene. These facts raise the question as to whether it would be possible to modify graphene to be an intrinsic superconductor.

Various theoretical attempts¹⁰⁻¹⁵ have been made to understand the superconductivity in graphene. Uchoa *et al.*¹⁰ suggested that an extended- s (ES) SC phase may be realized at the mean-field level due to the special structure of the honeycomb lattice. On the other hand, in a weak-coupling functional renormalization group study¹², Honerkamp found that with a nearest-neighbor (NN) spin-spin interaction J , doping away from half filling can lead to a $d + id$ SC state, which is similar to the SC state on the triangular lattice^{16,17}. This $d + id$ SC state was also found to be stable in a mean-field study¹³ of a phenomenological Hamiltonian¹⁴. Recent variational Monte Carlo simulations of the repulsive Hubbard model provide further support for the $d + id$ SC state¹⁵.

Although the results based on mean-field theory and other approximate methods are encouraging, it is far from certain that there exists a SC ground state in the physical parameter region of graphene. It is well known that the low energy properties of graphene can be described by the two-dimensional Hubbard model on a honeycomb lattice¹. In graphene, the on-site Hubbard repulsion is approximately half the band width, and this places graphene in an intermediate-coupling regime. Thus, it is questionable to approach the effect of electron correla-

tions in graphene from either a weak-coupling or strong-coupling limit, as was done in many previous theoretical studies. In view of the above-mentioned facts, we employ two accurate numerical methods, i.e., the determinant quantum Monte Carlo (DQMC)¹⁸ and constrained path Monte Carlo (CPMC) methods^{19,20}, to investigate possible electron correlation driven superconductivity in graphene.

Our extensive numerical simulations show that close to half filling, pairing with $d + id$ symmetry is dominant over pairing with ES symmetry. However, the long-range part of the $d + id$ pairing correlation tends to vanish in the thermodynamic limit, suggesting the absence of electron correlation driven superconductivity in our studied model. We also find that the NN interaction, either repulsive or attractive, does not enhance the tendency to the $d + id$ or ES superconductivity.

The structure of graphene can be described in terms of two interpenetrating triangular sublattices, A and B, and its low-energy electronic and magnetic properties can be well described by the extended Hubbard model on a honeycomb lattice¹,

$$H = -t \sum_{i\eta\sigma} a_{i\sigma}^\dagger b_{i+\eta\sigma} + \text{h.c.} + U \sum_i (n_{ai\uparrow} n_{ai\downarrow} + n_{bi\uparrow} n_{bi\downarrow}) + V \sum_{i\eta} n_{ai} n_{bi+\eta} + \mu \sum_{i\sigma} (n_{ai\sigma} + n_{bi\sigma}), \quad (1)$$

Here, $a_{i\sigma}$ ($a_{i\sigma}^\dagger$) annihilates (creates) electrons at site \mathbf{R}_i with spin σ ($\sigma = \uparrow, \downarrow$) on sublattice A, $b_{i\sigma}$ ($b_{i\sigma}^\dagger$) annihilates (creates) electrons at the site \mathbf{R}_i with spin σ ($\sigma = \uparrow, \downarrow$) on sublattice B, $n_{ai\sigma} = a_{i\sigma}^\dagger a_{i\sigma}$ and $n_{bi\sigma} = b_{i\sigma}^\dagger b_{i\sigma}$. $t \approx 2.5eV$ is the NN hopping integral and μ the chemical potential. $U \approx 6eV$ and V denote the on-site Hubbard interaction and NN interaction, respectively. We have mainly used $U = 3|t|$ and $V = 0$ in this Rapid Communication, except as explicitly noted otherwise.

Our numerical calculations are performed on lattices of double-48, double-75, double-108, and double-147 sites with periodic boundary conditions. The double-48 lat-

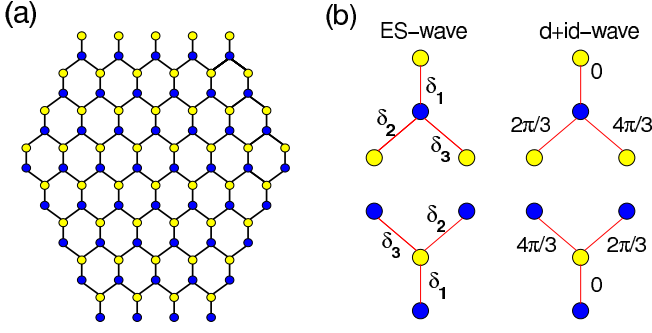


FIG. 1: (Color online) (a) Sketch of graphene with double-48 sites, (b) Phases of the $d + id$ and ES pairing symmetries on the honeycomb lattice. For clarity, the phase for the ES symmetry is omitted, which equals 0 for all δ_l .

tice is sketched in Fig. 1(a), where blue circles and yellow circles indicate the A and B sublattices, respectively. The system is simulated using DQMC at finite temperature and CPMC at zero temperature. The basic strategy of DQMC is to express the partition function as a high-dimensional integral over a set of random auxiliary fields. The integral is then accomplished by Monte Carlo techniques. In the CPMC method, the ground-state wave function is projected from an initial wave function by a branching random walk in an overcomplete space of constrained Slater determinants, which have positive overlaps with a known trial wave function. Extensive benchmark calculations showed that the systematic error induced by constraint is within a few percent and the ground-state observables are insensitive to the choice of trial wave function¹⁹. In our CPMC simulations, we employ closed-shell electron fillings and use the corresponding free-electron wave function as the trial wave function.

As magnetic excitation might play an important role in the SC mechanism of electronic correlated systems, we first study the magnetic correlations in graphene. Specifically, we compute the NN spin correlation $S_{\langle i,j \rangle}^{zz} = \langle S_i^z \cdot S_j^z \rangle$ and the spin structure factor $S(\mathbf{q})$, which is defined as,

$$S(\mathbf{q}) = \frac{1}{N_s} \sum_{d,d'=a,b} \sum_{i,j} e^{iq \cdot (i_d - j_{d'})} \langle m_{i_d} \cdot m_{j_{d'}} \rangle, \quad (2)$$

where $m_{i_a} = a_{i\uparrow}^\dagger a_{i\uparrow} - a_{i\downarrow}^\dagger a_{i\downarrow}$ and $m_{i_b} = b_{i\uparrow}^\dagger b_{i\uparrow} - b_{i\downarrow}^\dagger b_{i\downarrow}$. N_s denotes the number of sublattice sites.

To investigate the SC property of graphene, we compute the pairing susceptibility,

$$P_\alpha = \frac{1}{N_s} \sum_{i,j} \int_0^\beta d\tau \langle \Delta_\alpha^\dagger(i, \tau) \Delta_\alpha(j, 0) \rangle, \quad (3)$$

and the pairing correlation,

$$C_\alpha(\mathbf{r} = \mathbf{R}_i - \mathbf{R}_j) = \langle \Delta_\alpha^\dagger(i) \Delta_\alpha(j) \rangle, \quad (4)$$

where α stands for the pairing symmetry. Due to the constraint of the on-site Hubbard interaction in Eq. (1),

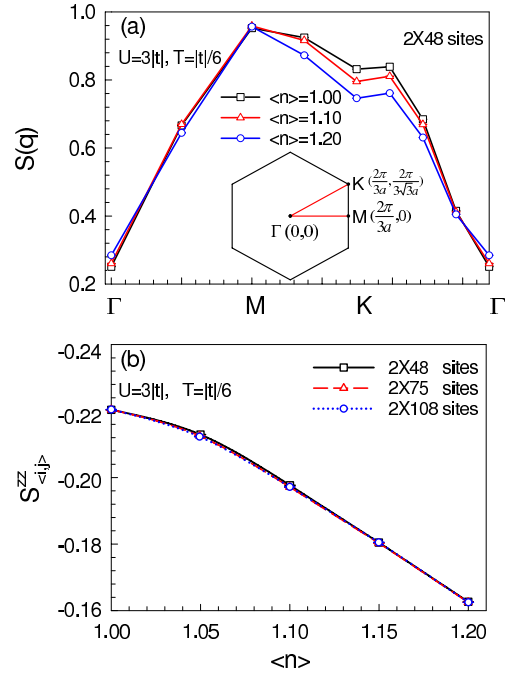


FIG. 2: (Color online) (a) Spin structure factor $S(\mathbf{q})$ on the double-48 lattice along the high symmetry lines in the first Brillouin zone (BZ) at electron fillings $\langle n \rangle = 1.00, 1.10, 1.20$. (b) NN spin correlation $S_{\langle i,j \rangle}^{zz}$ versus $\langle n \rangle$ on different lattices. The inset of (a) shows the first BZ, with a denoting the distance between NN lattice sites. The results are presented for temperature $T = |t|/6$.

pairing between two sublattices is favored and the corresponding order parameter $\Delta_\alpha^\dagger(i)$ is defined as

$$\Delta_\alpha^\dagger(i) = \sum_l f_\alpha^\dagger(\delta_l) (a_{i\uparrow}^\dagger b_{i+\delta_l\downarrow} - a_{i\downarrow}^\dagger b_{i+\delta_l\uparrow})^\dagger, \quad (5)$$

with $f_\alpha(\delta_l)$ being the form factor of pairing function. Here, the vectors δ_l ($l = 1, 2, 3$) denote the NN intersublattice connections, as sketched in Fig. 1(b). Considering that the pairing symmetry of graphene is governed by the $D6$ point group, two form factors for NN pairing described by the A_1 and E_2 irreducible representations of the $D6$ point group are given by¹¹,

$$ES\text{-wave} : f_{ES}(\delta_l) = 1, \quad l = 1, 2, 3 \quad (6)$$

$$d + id\text{-wave} : f_{d+id}(\delta_l) = e^{i(l-1)\frac{2\pi}{3}}, \quad l = 1, 2, 3 \quad (7)$$

In Fig. 2, we present the spin structure factor $S(\mathbf{q})$ and the NN spin correlation $S_{\langle i,j \rangle}^{zz}$ at different electron fillings for temperature $T = |t|/6$. A broad peak between M and K in Fig. 2(a) and a negative NN spin correlation in Fig. 2(b) indicate the existence of AFM spin correlation in graphene close to half filling. From Fig. 2(a), one can notice that even at half-filling, the peak is rather weak, suggesting that magnetic ordering is strongly frustrated due to the structure of the honeycomb lattice. Moreover, Fig. 2 shows that as the electron filling $\langle n \rangle$ increases

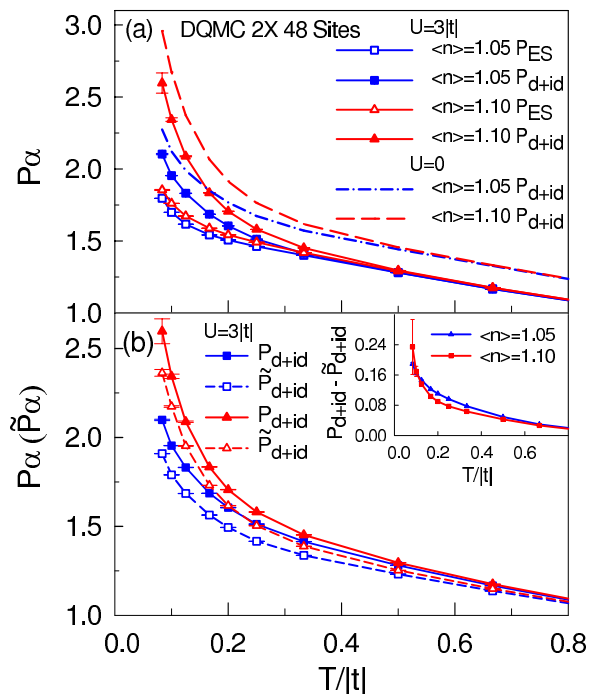


FIG. 3: (Color online) (a) Pairing susceptibility P_α as a function of temperature T for different pairing symmetries and different fillings, (b) \tilde{P}_{d+id} and P_{d+id} as a function of temperature at $\langle n \rangle = 1.05$ and $\langle n \rangle = 1.10$. Dashed and dashed-dotted lines in (a) represent the $d+id$ pairing susceptibility at $U=0$. The inset of (b) shows the effective pairing interaction $P_{d+id} - \tilde{P}_{d+id}$ as a function of temperature.

from half filling, $S(\mathbf{q})$ is reduced in the region around the K point and $S_{\langle i,j \rangle}^{zz}$ becomes less negative, which indicates that the AFM spin correlation is suppressed when the system is doped away from half filling. As it is expected that fermion systems with strong on-site repulsion may exhibit superconductivity induced by AFM spin fluctuations, and from the behavior of magnetic correlation shown in Fig. 2, it seems that the electron correlation driven superconductivity is possible through a similar mechanism in graphene. In the following, we discuss the behavior of pairing susceptibility and pairing correlation in the low doping region.

Figure 3 shows the temperature dependence of pairing susceptibilities for different pairing symmetries and electron fillings on the double-48 lattice. From Fig. 3(a), it is clear to see that within the filling range investigated, the pairing susceptibilities for both $d+id$ and ES pairing symmetries increase as the temperature is lowered. Most remarkable is that P_{d+id} increases much faster than P_{ES} at low temperatures. This demonstrates that the $d+id$ pairing symmetry is dominant over the ES pairing symmetry in the low doping region. In the whole temperature regime, one can observe that the value of P_{d+id} at $U=3|t|$ is smaller than the corresponding noninteracting one ($U=0$), as displayed in Fig. 3(a), which reflects the fact that the reduction of quasiparticle weight (self-

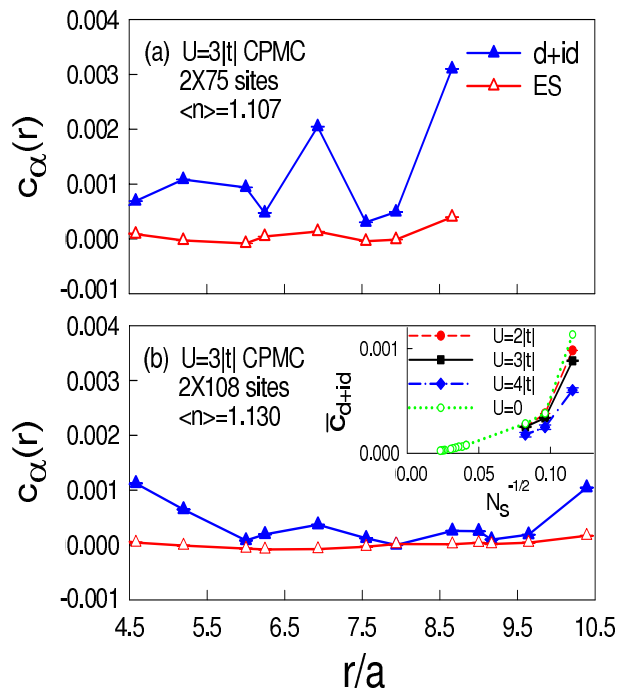


FIG. 4: (Color online) Pairing correlation C_α as a function of distance for the $d+id$ and ES pairing symmetries on the double-75 lattice with $\langle n \rangle = 1.107$ (a) and double-108 lattice with $\langle n \rangle = 1.130$ (b). The inset of (b) shows the average of the long-range $d+id$ pairing correlation \bar{C}_{d+id} vs $1/\sqrt{N_s}$ for different U 's at a filling $\langle n \rangle \approx 1.1$.

energy effect) due to electron correlation plays a negative role in enhancing the pairing susceptibility.

In order to extract the effective pairing interaction in different pairing channels, the bubble contribution $\tilde{P}_\alpha(i, j)$ is also evaluated, which is achieved by replacing $\langle a_{i\downarrow}^\dagger b_{j\uparrow} a_{i+\delta_{i\downarrow}}^\dagger b_{j+\delta_{i\uparrow}} \rangle$ with $\langle a_{i\downarrow}^\dagger b_{j\uparrow} \rangle \langle a_{i+\delta_{i\downarrow}}^\dagger b_{j+\delta_{i\uparrow}} \rangle$ in Eq. (3). In Fig. 3 (b), we plot both P_{d+id} and \tilde{P}_{d+id} for comparison. It is apparent that \tilde{P}_{d+id} shows a very similar temperature dependence to that of P_{d+id} . The effective pairing interaction, which can be estimated by the difference between P_{d+id} and \tilde{P}_{d+id} , is found to take a positive value and to increase with lowering temperature, as clearly shown in the inset figure. The positive effective pairing interaction indicates that there actually exists attraction for the $d+id$ pairing.

Based on the DQMC results for the pairing susceptibility, one expects that there may exist the $d+id$ SC state in the low-temperature region, which is manifested by a divergence of P_{d+id} at a certain temperature. Unfortunately, it is not clear whether the pairing susceptibility keeps growing at low temperatures since the sign problem prevents simulation in the low-temperature regime. In order to shed light on the critical issue as to whether there exists a long-range off-diagonal $d+id$ SC order in the ground state, we now turn to discuss the results obtained from the CPMC method.

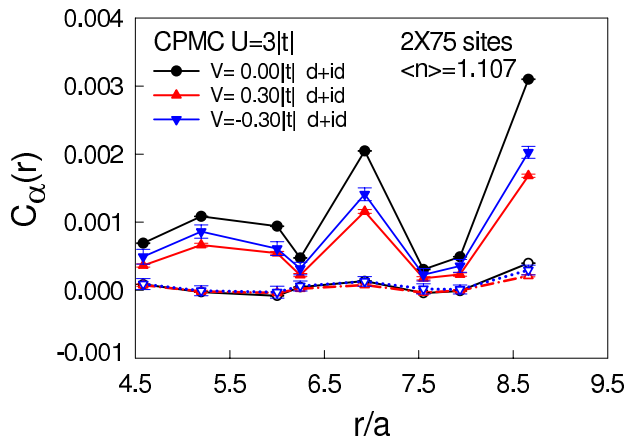


FIG. 5: (Color online) Pairing correlation as a function of distance for the $d+id$ (filled symbols) and ES (open symbols) pairing symmetries on the double-75 lattice with $\langle n \rangle = 1.107$. The value of NN interaction V is indicated by the shape of the symbol, which is also applied for the ES symmetry.

In Fig. 4, we compare the long-range part of pairing correlations for the $d+id$ and ES pairing symmetries on the double-75 and double-108 lattices, with a filling of approximately $\langle n \rangle = 1.1$. One can readily see that $C_{d+id}(r)$ is larger than $C_{ES}(r)$ for all long-range distances between electron pairs. Similar behavior is also observed on the double-147 lattice with $\langle n \rangle = 1.095$ (not shown here). This re-enforces our finding that the $d+id$ pairing symmetry dominates the ES pairing symmetry in the low doping region.

To gain insight into the behavior of the $d+id$ pairing correlation in the thermodynamic limit, we examine the evolution of C_{d+id} with increasing lattice size. In the inset of Fig. 4(b), the average of the long-range $d+id$ pairing correlation, $\overline{C}_{d+id} = \frac{1}{\sqrt{N'}} \sum_{r>4a} C_{d+id}(r)$, where N' is the number of electron pairs with $r > 4a$, is plotted as a function of $\frac{1}{\sqrt{N_s}}$ for $U = 0, 2|t|, 3|t|$, and $4|t|$. We observe that \overline{C}_{d+id} decreases as the lattice size increases, and shows a clear tendency to vanish in the thermodynamic limit ($\frac{1}{\sqrt{N_s}} \rightarrow 0$) at $U = 0$. This result, together with a decrease of \overline{C}_{d+id} with increasing U , suggests the absence of long-range $d+id$ SC order in the parameter regime investigated. Our finding is in agreement with the functional renormalization group study¹², where the SC instability does not occur in the doped Hubbard model. A similar decrease of \overline{C}_{d+id} with increasing lattice size

was also observed in the variational Monte Carlo calculations¹⁵. Thus, although AFM fluctuations can mediate a NN singlet pair, quantum fluctuations beyond the mean-field level shall destroy the phase coherence between electron pairs.

In graphene, the long-range interaction may also play a significant role on its physical properties, especially in the low doping region, where the long-range Coulomb interaction is not effectively screened because of a small density of state at the Fermi energy. We have studied the effect of NN interaction on the pairing correlation. In Fig. 5, the pairing correlations for both $d+id$ and ES pairing symmetries are displayed as a function of distance on the double-75 lattice with different NN interaction V 's. Here, we consider both repulsive and attractive NN interactions. We notice that the ES pairing correlation is hardly affected by the NN interaction, whereas the $d+id$ pairing correlation is suppressed by either a repulsive or attractive NN interaction. Our results are contrary to the finding of Uchoa *et al.*¹⁰, where the NN attraction can stabilize the ES SC state at the mean-field level. In addition, the inclusion of NN interaction does not enhance the tendency to the $d+id$ SC state. Therefore, we can conclude that within the extended Hubbard model, there seems to be an absence of SC order in the ground state.

In summary, we have studied the behavior of pairing correlation within the extended Hubbard model on a honeycomb lattice by using quantum Monte Carlo simulations. The results obtained from both DQMC and CPMC show that close to half filling, pairing with $d+id$ symmetry dominates pairing with ES symmetry, which is consistent with previous mean-field and functional renormalization group studies. This provides strong evidence that pairing with different spatial phases is favored for the AFM fluctuation mediated pairing interaction, which is similar to the case on the triangular lattice^{16,17}. However, the tendency of the $d+id$ pairing correlation to vanish in the thermodynamic limit suggests that electron correlation in graphene is not strong enough to produce an intrinsic superconductivity. In an induced SC state by the proximity effect through a connection to another superconductor, the dominant $d+id$ pairing could be manifested in the unique properties of the SC gap function and the Andreev conductance spectra¹¹.

This work is partially supported by HKSAR RGC Project No. CUHK 402310. Z.B.H was supported by NSFC Grant No. 10974047.

* Electronic address: huangzb@hubu.edu.cn

† Electronic address: hqlin@phy.cuhk.edu.hk

¹ A. H. Castro Neto, F. Guinea, N. M. R. Peres, K. S. Novoselov and A. K. Geim, Rev. Mod. Phys, **81**, 109 (2009).

² K. S. Novoselov, A. K. Geim, S. V. Morozov, D. Jiang, M.

I. Katsnelson, I. V. Grigorieva, S. V. Dubonos and A. A. Firsov, Nature **438**, 197 (2005); Yuanbo Zhang, Yan-Wen Tan, Horst L. Stormer and Philip Kim, Nature **438**, 201 (2005).

³ Z. Y. Meng, T. C. Lang, S. Wessel, F. F. Assaad and A. Muramatsu, Nature **464**, 847 (2010).

- ⁴ S. Raghu, X.-L. Qi, C. Honerkamp, and S.-C. Zhang, Phys. Rev. Lett. **100**, 156401 (2008).
- ⁵ Guohong Li, A. Luican, J. M. B. Lopes dos Santos, A. H. Castro Neto, A. Reina, J. Kong and E. Y. Andrei, Nature physics **6**, 109 (2010).
- ⁶ Tianxing Ma, Feiming Hu, Zhongbing Huang and Hai-Qing Lin, Appl. Phys. Lett **97**, 112504 (2010).
- ⁷ N. M. R. Peres, M. A. N. Araujo, and Daniel Bozi, Phys. Rev. B **70**, 195122 (2004).
- ⁸ T. Paiva, R. T. Scalettar, W. Zheng, R. R. P. Singh, and J. Oitmaa, Phys. Rev. B **72**, 085123 (2005).
- ⁹ H. B. Heersche, P. Jarillo-Herrero, J. B. Oostinga, L. M. K. Vandersypen, and A. F. Morpurgo, Nature **446**, 56(2007); F. Miao, S. Wijeratne, Y. Zhang, U. C. Coskun, W. Bao, and C. N. Lau, Science **317**, 1530(2007); X. Du, I. Skachko, and E. Y. Andrei, Phys. Rev. B **77**, 184507 (2008).
- ¹⁰ B. Uchoa and A. H. Castro Neto, Phys. Rev. Lett. **98**, 146801 (2007).
- ¹¹ Y. Jiang, D.-X. Yao, E. W. Carlson, H.-D. Chen, and J. P. Hu, Phys. Rev. B **77**, 235420 (2008).
- ¹² C. Honerkamp, Phys. Rev. Lett. **100**, 146404 (2008).
- ¹³ A. M. Black-Schaffer and S. Doniach, Phys. Rev. B **75**, 134512 (2007).
- ¹⁴ G. Baskaran, Phys. Rev. B **65**, 212505 (2002).
- ¹⁵ S. Pathak, V. B. Shenoy, and G. Baskaran, Phys. Rev. B **81**, 085431 (2010).
- ¹⁶ B. Kumar and B. S. Shastry, Phys. Rev. B **68**, 104508 (2003).
- ¹⁷ Qiang-Hua Wang, Dung-Hai Lee, and Patrick A. Lee, Phys. Rev. B **69**, 092504 (2004); Sen Zhou, and Ziqiang Wang, Phys. Rev. Lett. **100**, 217002 (2008).
- ¹⁸ R. Blankenbecler, D. J. Scalapino, and R. L. Sugar, Phys. Rev. D **24**, 2278 (1981).
- ¹⁹ S. W. Zhang, J. Carlson and J. E. Gubernatis, Phys. Rev. Lett. **74**, 3652 (1995); Phys. Rev. B **55**, 7464 (1997).
- ²⁰ Z. B. Huang, H. Q. Lin and J. E. Gubernatis, Phys. Rev. B **64**, 205101 (2001); *ibid.* **63**, 115112 (2001).